Published in final edited form as:

Mol Microbiol. 2004 May ; 52(3): 661–675. doi:10.1111/j.1365-2958.2004.04005.x.

Specific recognition of *rpsO* mRNA and 16S rRNA by *Escherichia coli* ribosomal protein S15 relies on both mimicry and site differentiation

Nathalie Mathy[1], **Olivier Pellegrini**[1], **Alexander Serganov**[2], **Dinshaw J. Patel**[2], **Chantal Ehresmann**[3], and **Claude Portier**[1,*]

[1]UPR9073 du CNRS, Institut de Biologie Physico-Chimique, 13 rue Pierre et Marie Curie, 75005 Paris, France

[2]Laboratory of Nucleic Acid and Protein Structures, Memorial Sloan-Kettering Cancer Center, 1275 York Avenue, New York, NY 10021, USA

[3]UPR9002 du CNRS, Institut de Biologie Moléculaire et Cellulaire, 15 rue René Descartes, 67084 Strasbourg cedex, France

Summary

The ribosomal protein S15 binds to 16S rRNA, during ribosome assembly, and to its own mRNA (*rpsO* mRNA), affecting autocontrol of its expression. In both cases, the RNA binding site is bipartite with a common subsite consisting of a G•U/G-C motif. The second subsite is located in a three-way junction in 16S rRNA and in the distal part of a stem forming a pseudoknot in *Escherichia coli rpsO* mRNA. To determine the extent of mimicry between these two RNA targets, we determined which amino acids interact with *rpsO* mRNA. A plasmid carrying *rpsO* (the S15 gene) was mutagenized and introduced into a strain lacking S15 and harbouring an *rpsO–lacZ* translational fusion. Analysis of deregulated mutants shows that each subsite of *rpsO* mRNA is recognized by a set of amino acids known to interact with 16S rRNA. In addition to the G•U/G-C motif, which is recognized by the same amino acids in both targets, the other subsite interacts with amino acids also involved in contacts with helix H22 of 16S rRNA, in the region adjacent to the three-way junction. However, specific S15–*rpsO* mRNA interactions can also be found, probably with A(−46) in loop L1 of the pseudoknot, demonstrating that mimicry between the two targets is limited.

Introduction

Many macromolecules can specifically bind more than one partner, because several distinct binding sites are present in these molecules. For example, 16S and 23S rRNAs bind to numerous ribosomal proteins, and RNase E associates with other enzymes to constitute the ‘degradosome’ (Vanzo *et al*., 1998). In a few cases, however, macromolecules can bind different partners alternately, suggesting that some structural mimicry may exist between the different ligands. This situation is illustrated in *Escherichia coli* by the binding of $tRNA^{Thr}$

*For correspondence. portier@ibpc.fr; Tel. (+33) 1 58 41 51 27; Fax (+33) 1 58 41 50 20.

and the *thrS* mRNA to threonyl-tRNA synthetase (ThrRS). In fact, this translational operator mimics the structure of well-defined parts of $tRNA^{Thr}$ (Torres-Larios *et al*., 2002; Romby and Springer, 2003) to allow autocontrol of ThrRS translation (Springer *et al*., 1985). The recognition of RNA targets by the ribosomal protein S15 is more complex as the substrates share only partial similarity. This small evolutionarily conserved protein binds to a highly conserved region in the central domain of 16S rRNA. S15 interactions were studied extensively in *Bacillus stearothermophilus* (Batey and Williamson, 1996a,b; Scott and Williamson, 2001), *E. coli* (*Ec*) (Serganov *et al*., 2001 and references therein) and *Thermus thermophilus* (*Tt*) (Serganov *et al*., 1996; 1997). Two subsites of 16S rRNA recognition were characterized. The major subsite is a three-way junction between helices H20, H21 and H22, restrained by an invariant C-G•G base triple (Agalarov *et al*., 2000; Nikulin *et al*., 2000; Serganov *et al*., 2001). The minor subsite, located one helical turn from the three-way junction in helix H22, consists of a conserved G•U/G-C motif (Fig. 1) (Batey and Williamson, 1996; Serganov *et al*., 1996; 2001; 2002; 2003).

Ec-S15 and *Tt*-S15 also bind specifically to their own mRNAs to control their own expression negatively (Portier *et al*., 1990; Philippe *et al*., 1993; Serganov *et al*., 2003). Although these mRNA binding sites are also bipartite, they do not share any obvious similarities, but appear to mimic some of the rRNA subsites. The *Tt-rpsO* mRNA shares sequence and structural similarity with the *Tt*-rRNA three-way junction (including the C-G•G base triple), but lacks the G•U/G-C motif (Serganov *et al*., 2003), whereas the *Ec-rpsO* mRNA target does not fold into a three-way junction but rather into a pseudoknot that contains a G•U/G-C motif (Fig. 1). As *Ec*-S15 recognizes this pseudoknot with a lower affinity than 16S rRNA, it was possible that the presence of the G•U/G-C motif was sufficient for S15 recognition. However, *in vivo* and *in vitro* experiments have shown that this is not the case (Bénard *et al*., 1998; Serganov *et al*., 2002). A second subsite, provided by the pseudoknot itself, is also required for *Ec*-S15 binding, despite the lack of sequence similarity with the major binding site of *Ec*-16S rRNA (Bénard *et al*., 1994; Serganov *et al*., 2002). These observations suggest that only a partial mimicry exists between *Ec-rpsO* mRNA and *Ec*-16S rRNA. Moreover, although protein footprinting assays clearly demonstrate that the protein uses the same surface for recognition of both RNA targets (Serganov *et al*., 2002), no amino acids involved in mRNA binding have being identified until now. Thus, the model of the *Ec*-S15–pseudoknot complex, postulating that the G•U/G-C motif is recognized by the same amino acids of S15 in both targets (Serganov *et al*., 2002), required experimental support. In this paper, we developed an *in vivo* assay that allowed us to isolate S15 mutations affecting the S15–*rpsO* mRNA interaction without altering 30S subunit assembly. The results obtained provide insights into the role of individual amino acids in the recognition of two RNAs by S15.

Results

Strategy

To identify *Ec*-S15 amino acids critical for mRNA binding *in vivo*, two independent mutagenesis experiments were performed. The first consisted of the introduction of specific mutations in predetermined positions of *rpsO*, the *Ec*-S15 gene, whereas the second

consisted of random mutagenesis of the *rpsO* gene. Experiments were based on the premise that preventing S15 from binding to its mRNA would result in a loss of autocontrol, leading to S15 overexpression (Philippe *et al*., 1990; Portier *et al*., 1990). The effect of the S15 mutations was followed by inserting a *rpsO–lacZ* translational fusion into the chromosome of a Δ*lac* strain (Portier *et al*., 1990) and measuring the level of β-galactosidase after transformation of the strain with a plasmid carrying the mutagenized *rpsO* gene (Fig. 2). To avoid competition between the wild-type S15 produced by the chromosomal copy of *rpsO* gene and S15 mutants expressed from the plasmid, a Δ*rpsO* deletion was introduced into the Δ*lac* strain carrying the *rpsO–lacZ* translational fusion (see *Experimental procedures*). This strain, named CPFΔS15, was cold sensitive at 30°C, but grew at 42°C, with a generation time of around 100 min. Thus, active ribosomes can be synthesized in the absence of S15 at 42°C, consistent with previous observations (Ferro-Novick *et al*., 1984; Yano and Yura, 1989). The cold sensitivity phenotype could be complemented by transformation with any plasmid expressing an active S15 protein, such as pRPSO. This plasmid carried the wild-type *rpsO* gene under the control of p *Trc*, an IPTG-inducible promoter. Without inducer, transcription of the *rpsO* gene was strongly repressed by the Lac repressor synthesized from the $lacI^q$ gene (Fig. 2), whereas the addition of IPTG triggered S15 expression and allowed bacteria to grow at 30°C. As the highest growth rate was reached at an IPTG concentration of 10^{-4} M (data not shown), this concentration was used for all subsequent experiments.

Expression of the *rpsO–lacZ* fusion in the presence of wild-type S15 repressor

Cells lacking S15 (strain CPFΔS15 with or without the plasmid control pTrc99A) were grown at 42°C. Under these conditions, around 10^4 units of β-galactosidase were synthesized (Table 1), a value corresponding to full derepression of the fusion. After transformation with plasmid pRPSO, the β-galactosidase level dropped significantly in cells grown at 42°C (46 ± 7 units) (Table 1). These data provide a measure of the repression of the *rpsO–lacZ* fusion by wild-type S15 (R in Table 1).

Site-directed mutagenesis of the ribosomal protein S15

Mutagenesis of amino acids interacting with 16S rRNA—In the first set of experiments, several amino acids (circles, Fig. 3) interacting with the minor and major binding sites of 16S rRNA (Agalarov *et al*., 2000; Nikulin *et al*., 2000) were changed by site-directed mutagenesis and introduced into the plasmid-borne *rpsO* gene. The effect of these mutations was analysed by measuring β-galactosidase levels in strain CPFΔS15 transformed by these plasmids. The data are given in Table 1.

Residues interacting with the G•U/G-C site. *Tt*-S15 specifically recognizes the minor groove bases of nucleotides in the G•U/G-C motif of the 16S rRNA via three conserved amino acids, His-41, Asp-48 and Ser-51 (Fig. 1; Table 1) (Agalarov *et al*., 2000; Nikulin *et al*., 2000). The side-chains of His-41 and Asp-48 form hydrogen bonds with the functional groups of the G667–C739 pair, whereas Ser-51 contacts the G666–U740 pair via a water molecule. Replacement of His-41 and Asp-48 by amino acids with shorter side-chains (Ala and Gly respectively) induced a total loss of autocontrol (Table 1). This is consistent with the fact that inversion or substitution of the G(−35)C(−50) pair in the *rpsO* mRNA, the potential analogue of the G667–C739 pair in 16S rRNA, results in a loss of S15 binding and

autocontrol (Bénard *et al*., 1998; Serganov *et al*., 2002). Therefore, His-41 and Asp-48 probably recognize the G-C pair of the G•U/G-C motif similarly to rRNA. Unexpectedly, the replacement of Ser-51 by Ala did not affect regulation (Table 1). This change, resulting in the substitution of a hydroxyl group by a hydrogen atom, should have been sufficient to disrupt specific interactions of Ser-51 with both U(−49) and G(−36), if the same interactions existed in the mRNA. On the other hand, the loss of regulation caused by replacement of Ser-51 with Leu suggests that Ser-51 is indeed in close proximity to G(−49)U(−36). The bulky side-chain of Leu more than likely causes a steric clash with the neighbouring RNA. Remarkably, this effect is consistent with the fact that substitution of G(−36) by inosine (an analogue of G lacking the exocyclic N2 group) and of U(−49) by dT had only a minor effect on the binding affinity of the mRNA pseudoknot for *Ec*-S15, again indicating that there is no direct contact with the G•U pair (Serganov *et al*., 2002). Taken together, these observations indicate that the G•U/G-C motif in mRNA is recognized by *Ec*-S15 in a similar, but not strictly identical, manner to 16S rRNA. Consistent with this observation, the structural environment of this motif is different in both RNAs. In the mRNA, it is flanked by classical Watson–Crick pairs, whereas in 16S rRNA, it is adjacent to G•A pairs and a bulging A residue (Agalarov *et al*., 2000; Nikulin *et al*., 2000). In this line, Gln-34, which contacts the phosphate group of the *Tt*-rRNA G742 between the two G•A pairs, could be substituted by Ala without changing the repression level (Fig. 1; Table 1), thus accounting for a difference in backbone conformation between the two RNA targets.

Residues interacting in the three-way junction. Recognition of the major binding site in 16S rRNA occurs via an extended network of interactions defined by the unique geometry of the RNA three-way junction. As a consequence, contacts are essentially made between the sugar–phosphate backbone of RNA and S15 residues that are only moderately conserved (Agalarov *et al*., 2000; Nikulin *et al*., 2000). The K64A, Y68A and R71A mutations, which affect amino acids involved in recognition of the three-way junction in 16S rRNA (Nikulin *et al*., 2000), had no significant effect on autocontrol (Table 1). As the three-way junction is lacking in *rpsO* mRNA, the lack of effect of these mutations on autorepression indicates that no structural equivalent of the junction is built into the mRNA.

In addition to the specific recognition of the geometry of the three-way junction backbone, contacts were also observed between S15 and the poorly conserved part of helix H22 of *Tt*-16S rRNA, adjacent to the three-way junction. These contacts mainly involve functional groups within the minor groove (Fig. 1; Table 1). Thus, amino acids Thr-21, Gly-22 and Gln-27, which interact with C656–G750/G657–C749 in *T. thermophilus* (Nikulin *et al*., 2000) and G656–C750/U657–A749 in *E. coli* (Serganov *et al*., 2001), were mutated. The T21A, G22A, Q27A and Q27R mutations all resulted in either strong (Q27A and Q27R) or complete (T21A and G22A) derepression (Table 1). Alanine substitutions of Thr-4 and Thr-7, two other potential candidates for minor groove binding, had a weak effect on autocontrol (Table 1), suggesting that they contribute only moderately to the stability of the S15–mRNA complex. In contrast, Thr-24, which interacts with U751(O2′) in 16S rRNA, could be substituted by Ala or Ser without affecting regulation. Taken together, these observations suggest that a subset of amino acids, which recognize the minor groove of helix H22 in *Ec*-16S rRNA, are involved in the recognition of a corresponding helical portion of

the mRNA pseudoknot. Despite the absence of sequence similarity, this region presumably corresponds to stem S2 of the pseudoknot, stacked under stem S1 in Figs 1 and 6B. This is supported by hydroxyl radical footprinting data, which identified a second subsite in stem S2 in this area, in addition to the G•U/G-C motif in stem S1 (Philippe *et al*., 1995; Serganov *et al*., 2002) (Fig. 1).

Mutagenesis of amino acids not involved in the S15–16S rRNA interaction

In the second set of experiments, several residues of S15 not involved in 16S rRNA recognition were mutated in the hope of identifying amino acid(s) specifically involved in mRNA recognition. The model of the S15–mRNA complex (Serganov *et al*., 2002) was used to select which amino acids to mutate. As a control, three amino acids (Arg-52, Ser-60 and Arg-83) predicted to be far from mRNA in the model, were mutated to alanine. Consistent with the predictions, these mutations had no effect on autocontrol (Table 1, R52A, S60A and R83A). Other amino acids, such as Leu-38, Arg-57 or Gln-61, which are located near mRNA in the S15–mRNA complex, were also mutated. The Q61A mutation had no effect, excluding a possible interaction between Gln-61 and A(−46). The L38N mutation resulted in a loss of autocontrol, while the L38A mutation caused a weaker deregulation (Table 1). These results suggested a conformational defect rather than a loss of contact with mRNA. However, the effect of the L38A mutation was greater than that observed in other similar cases (see L56A, Q39A in Table 1). Another mutation near mRNA, R57A, also induced a strong derepression of fusion expression. Polar residues, such as Asn and Gln, had the same effect, while repression was partially restored by substitutions by a positively charged amino acid (Lys) or, to a lesser extent, His (Table 1). This suggests that a basic residue is required at position 57. Interestingly, the location of the positively charged residue is not absolutely critical, as demonstrated by a significant improvement in the repression factor (from 2 to 46 at 30°C and from 1 to 7 at 42°C) in the presence of the double R57A–M58K mutation. Thus, the negative effect on the repression efficiency induced by the R57A mutation can be partly compensated for by a positively charged Lys at the adjacent position 58. The single mutation M58K, which placed two positively charged residues side by side, did not improve the efficiency of autocontrol. These results strongly suggest that S15 binding to mRNA requires specific contacts made by amino acids that are not involved in the S15–16S rRNA interaction.

Random mutagenesis

To identify additional amino acids that might be specifically involved in mRNA binding, we also randomly mutagenized the *rpsO* gene. The plasmid-borne *rpsO* gene was mutagenized by polymerase chain reaction (PCR) (see *Experimental procedures*), and the resulting PCR fragments were digested with *Nco*I and *Sal*I and transferred to another plasmid cut with the same enzymes. The plasmid pools were further transferred into the CPFΔS15 strain, and blue colonies were selected on indicator plates at 30°C. At this temperature, blue clones should contain mutations affecting the mRNA-binding properties of S15, but not the ability of S15 to form ribosomes. The number of mutations per *rpsO* gene varied from 1 to 12. Some mutations did not change the amino acid sequence of S15 because they occurred in the wobble position (data not shown). In some other cases, dissection of multiple mutations by

site-directed mutagenesis allowed us to identify which residues were responsible for the phenotype observed.

Single mutations

Of the single mutations (squares, Fig. 3), some caused no significant (L2P, Y68N and Y77C) or only a moderate (L80F) increase in fusion expression (Table 1), suggesting that these amino acids are not directly involved in S15–mRNA binding. Of those mutations affecting autocontrol, only one (T21A) had already been analysed by site-directed mutagenesis (see above). Other point mutations, F14S, F14L, Q39L and L56P, which also abolish autocontrol, were found at positions not predicted to contact 16S rRNA. Two of these mutations, Q39L and L56P, are likely to disrupt contacts made by the neighbouring residues, Leu-38 and Arg-57. Consistent with this hypothesis, a proline cannot be accommodated at position 56 in the model of the complex, without local distortion of the backbone, which would change the position of the adjacent Arg-57, essential for autocontrol. Similarly, the Q39L mutation, which places a bulky hydrophobic residue instead of a polar amino acid next to Leu-38, had a more dramatic effect than Q39A, where Gln-39 was replaced by an amino acid with a small side-chain (Table 1). F14S and F14L mutations have the same strong negative effect on autocontrol (data not shown). This effect is probably not caused by loss of contact, but rather a conformational defect or/and decreased stability (see below), as Phe-14 is located far from the mRNA in the proposed model of the complex.

Multiple mutations

Several other mutants that cause deregulation of fusion expression carried multiple mutations (data not shown). Among them, mutations already known to abolish autocontrol were often present (e.g. at positions 21 and 22). With some other multiple mutants, all of which had the G15A mutation in common, the cultures stopped growing after two generations at 42°C. This G15A mutation was then made by site-directed mutagenesis and introduced into strain CPFΔS15. When these cells were cultured at 42°C, growth also stopped after two generations (Fig. 4), showing that growth arrest results solely from the G15A mutation. Interestingly, when expression of the fusion was measured at 30°C in the presence of this mutation, only a weak effect on the repression efficiency was observed (Table 1). Two other multiple mutants deserve special attention. In the first, deletion Δ82–88, which removed the C-terminal part of helix α4, caused a partial derepression of fusion expression (Table 1). In the model of the S15–mRNA complex, this helix is located on the face opposite that interacting with RNA, suggesting that the limited effect observed corresponds to a local destabilization of the S15 structure upon removal of this portion of helix α4. In the second mutant, a combination of five mutations (K9R, I35V, H37R, F42L and E82D) decreased repression efficiency only slightly (106 ± 2 units at 30°C and 275 ± 4 at 42°C), suggesting that none of these amino acids interact with *rpsO* mRNA. In summary, the random mutagenesis data confirmed and extended the results obtained by site-directed mutagenesis. It provided further evidence that amino acids such as Tyr-68, which is involved in recognition of the three-way junction in 16S rRNA, do not participate in mRNA recognition. Most other residues identified by this technique were already known to interact

with rRNA (e.g. Gly-22 and Thr-21) or to be adjacent to residues suspected to be in contact solely with mRNA (e.g. Glu-39 and Leu-56).

Binding affinity of S15 mutants

We tested next whether a drop in repression efficiency could be correlated with a decrease in the binding affinity for *rpsO* mRNA. The apparent dissociation constants (K_d) of selected S15 mutants for mRNA were measured using an *in vitro* filter-binding assay. The S15 mutant proteins carrying the F14L, R57A, R57K, R57K/M58K and M58K mutations were purified from *Ec* cells, and their binding affinities for three different RNAs were determined: the minimum pseudoknot mRNA45 (Serganov *et al*., 2002), a 16S rRNA fragment and an unrelated RNA (tmRNA). The results are given in Table 2. All S15 mutants bound the control RNA with very low affinity (>10 μM). As expected, the F14L mutation decreased more strongly the S15 affinity for mRNA than for rRNA (14-fold versus three-fold), accounting for the deregulation observed *in vivo*. Similarly, the R57A mutation significantly lowered the binding affinity for mRNA (27-fold), while only affecting 16S rRNA binding by fourfold. The R57K and R57A/M58K mutations were tolerated for rRNA, but not for mRNA binding, although a 46-fold repression factor was observed *in vivo* at 30°C. The M58K mutation increased the affinity for both rRNA (threefold) and mRNA (sevenfold), indicating that a lysine, when adjacent to R57, might interact with the mRNA pseudoknot. However, this increased affinity did not correlate with an increase in the repression efficiency. To check whether this absence of effect on *in vivo* repression could be explained by saturation of the *rpsO* mRNA with the protein, we decreased the amount of S15 in the cell by decreasing the concentration of IPTG to 10^{-5} M. This resulted in a 20-fold lower repression efficiency for both wild-type S15 and the M58K mutant (data not shown), indicating that the mutant protein is not more efficient than wild-type S15 in repressing fusion expression. Taken together, the *in vitro* binding assays confirmed the *in vivo* results and showed that several mutations that deregulate S15 expression strongly affect the affinity of S15 for mRNA, without a significant effect on 16S rRNA. Furthermore, autocontrol does not appear to be limited by the affinity of S15 for *rpsO* mRNA as the regulation efficiency is not improved by a mutation that increases its binding affinity.

Stability of mutant S15 proteins

It was possible that some point mutations might lead to S15 instability in the cell, resulting in low intracellular levels and an apparent loss of autocontrol, without affecting the affinity of S15 for mRNA. To estimate the decay rates of the different S15 mutants *in vivo*, cells were grown in the absence of IPTG at 42°C until the optical density at 650 nm reached 0.5. S15 production was then induced by ITPG, and transcription and translation were stopped after 30 min by the addition of rifampicin and chloramphenicol. The amount of S15 was measured by immunoblots. A plot of the amount of S15 versus time showed that decay occurred rapidly for the first 30 min and then slowed down (Fig. 4). This biphasic curve could be explained by the presence of two populations of S15: (i) a major, rapidly, decaying fraction, likely to correspond to free S15 or to S15 associated with mRNA; (ii) a minor, slowly, decaying population, likely to be trapped within the ribosome. Indeed, as the period of S15 synthesis was short (30 min) compared with the generation time (around 100 min), only a small fraction of S15 can have been incorporated into 30S particles, accounting for

the low level of the ‘stable’ S15 fraction. The same experiments, conducted with the T21A, H41A, D48G, S51L, R57A, R57Q and Δ82–88 mutants, showed that their decay rate was slightly slower than that of the pRPSO-borne S15 (data not shown). The sole exception was the mutant carrying the F14S mutation, which decayed about twofold faster than wild-type S15. Consistent with this observation, the amount of this mutant was twofold lower than that of the control (or of other mutants). In addition, the migration rate of the F14S mutant protein was also slower than the control (Fig. 5, inset). This result suggests that this mutation causes a significant conformational change in the protein S15, which might account for both its instability and its loss of repression efficiency. This defect probably results from the strategic position of this hydrophobic residue, conserved in *Ec*- and *Tt*-16S rRNA, in the proximity of Ala-29 (in helix α2), and L80 and L84 (in helix α4) (Fig. 3), which participate in the overall cohesion of the three-dimensional structure of the protein.

Interestingly, the initial decay of the M58K mutant was identical to wild-type S15, but an extremely slow degradation phase was detected after 20 min, suggesting that a significant amount of the R57K mutant was protected from degradation. Whether this protection results from tighter association of S15 to the ribosomes as a result of the increased affinity of this mutant for 16S rRNA remains to be determined.

Similar results were obtained when cells were grown at 30°C. However, in this case, the decay rates levelled off faster, making measurements more difficult and less accurate (data not shown).

Model of S15–mRNA complex

Taking into account the data presented above, we have improved the three-dimensional model of the S15–mRNA complex proposed previously (Serganov *et al*., 2002). The potential contacts between *Ec*-S15 and the mRNA pseudoknot are shown in Fig. 6A and B, and the improved model of the complex is shown in Fig. 6C. In this model, amino acids specifically involved in the recognition of the backbone geometry of the three-way junction do not recognize the mRNA pseudoknot, confirming that no structural equivalent of this site is present in the mRNA. On the other hand, the recognition of the G•U/G-C motif, present in both rRNA and mRNA and known to be an essential determinant of mRNA recognition, involves common amino acids in both cases (His-41, Asp-48 and Ser-51). Amino acids Gly-22, Gln-27 and Thr-21, which are conserved in *Tt*-S15 and interact with two adjacent basepairs (G750–C656 and C749–G657) in helix H22 of *Tt*-16S rRNA (Figs 1 and 6, Table 1) (Agalarov *et al*., 2000; Nikulin *et al*., 2000), are also involved in autoregulation. The model indicates that Gln-27 and Thr-21 can potentially contact the U(−45)A(+10) basepair in the distal part of stem S2 (Table 1, Fig. 6). Although not very far from the mRNA stem S2, Gly-22 does not make direct contact with mRNA. It is likely that loop 1 of *Ec*-S15, which contains Phe-14, adopts a different conformation from that of *Tt*-S15, as a result of differences in amino acid sequence (Fig. 3). This highlights a limit of modelling, as changing a protein loop is very speculative in the absence of structural data. The assumption that *Ec*-S15 loop 1 exhibits a specific conformation is further supported by the fact that the G15A mutation, which introduces the alanine residue found in *Tt*-S15, leads to a

thermosensitive phenotype. Thus, we think that Gly-22 probably makes a contact with stem S2, but we have been unable to define its RNA partner.

Thr-4 and Thr-7 also appear to contribute, albeit weakly, to autocontrol. These amino acids are the equivalents of Lys-4 and Lys-7 in *Tt*-S15, which contact the phosphate groups of G660 and G658 respectively. In its current form, the model does not allow us to identify unequivocal contact, i.e. within hydrogen bond distance, but suggests a contact with the minor groove of stem S2. Thus, it turns out that amino acids that recognize the minor groove of helix H22 in 16S rRNA are used to contact the distal part of stem S2 in the pseudoknot. It is worth noting that this site is separated from the G•U/G-C motif by 8 bp in both rRNA and mRNA, and its position correlates with data from footprinting experiments (Philippe *et al*., 1995; Serganov *et al*., 2002).

As our results show that A(−46) and Arg-57 are essential residues for *Ec*-S15 mRNA recognition, we used modelling to test whether a specific contact might occur between these residues. In the initial model, A(−46) was bulged out from the co-axially stacked stems S1 and S2, thus accounting for the reactivity of this nucleotide to chemical probes. However, in the absence of additional data, its orientation was arbitrary. Similarly, the lateral chain of Arg-57 (a methionine in *Tt*-S15) was also modelled in an arbitrary orientation. Only a slight movement of the bulged A(−46) and the lateral chain of Arg-57 is required to create a novel specific contact. Thus, in the new model, the lateral chain of Arg-57 is stacked on the adenine ring of A(−46) and makes a hydrogen bond with its phosphate group (Fig. 6C). A similar stacking interaction has been observed between Arg-53 and the purine ring of A728 in the *Tt*-S15–rRNA complex (Agalarov *et al*., 2000). This kind of interaction might account for the fact that it is possible to substitute Arg-57 with lysine, histidine or asparagine (Table 1). Consistent with this hypothesis, A(−46) can be replaced by guanine, but not by cytosine *in vivo*, without affecting autocontrol (Bénard *et al*., 1994). Moreover, substitution of A(−46) by deoxyadenosine can be tolerated while deletion of the adenine residue or substitution by a deoxyribose phosphate spacer missing the base ring abolishes S15 binding (Serganov *et al*., 2002).

Discussion

We have successfully constructed, for the first time, a strain completely lacking S15, a primary rRNA-binding protein. Like other strains lacking ribosomal proteins essential for ribosome assembly and exhibiting temperature sensitivity (Dabbs, 1991), this strain is cold sensitive and dies after a short time at 4°C, presumably because ribosomes cannot be assembled at low temperature. Interestingly, of all the mutations created, only one, G15A, exhibited a clear thermosensitive phenotype. This change probably does not prevent S15 binding to 16S rRNA at high temperature, as ribosomes can be synthesized at 42°C without S15. We conclude that this mutation affects 30S particle assembly or ribosome activity at high temperature, but affects mRNA binding much less so, as shown by the weak effect on autocontrol. In all cases but one (the G22A mutant grown at 30°C), the growth rate was not affected, indicating that ribosome assembly still occurred and suggesting that the overall translation rate was not modified. Notably, mutations affecting amino acids such as Gln-27, Tyr-68 and Arg-71 that contact the three-way junction in the major binding site of the 16S

rRNA still sustained growth at both high and low temperature. The synthesis of large amounts of S15 upon addition of IPTG would be predicted to compensate for small decreases in the binding affinity for 16S rRNA, leading to incorporation of S15 in 30S particles (data not shown) and growth at 30°C. On the other hand, high levels of S15 would also be predicted to saturate its mRNA target, obscuring any limited change in the amount of S15 or in its binding affinity. Consistent with this hypothesis, a constant low expression level of the fusion is always observed, even when S15 is overproduced (this study; Portier *et al*., 1990) or exhibits a higher affinity for its mRNA target (R57A/M58K mutation).

We considered the possibility that the ribosomal protein pools might be affected by degradation. Although the deg radation of the ribosomal proteins has been known for a long time and is stimulated when the proteins are overproduced (Olsson and Isaksson, 1979; Nishi and Schnier, 1988; Petersen, 1990), this effect should not be strong enough to prevent the saturation of mRNA targets, particularly in the system described in this paper. In these experiments, *rpsO* is strongly expressed, and the sole S15 mRNA target is the chimeric *rpsO–lacZ* mRNA. Moreover, the degradation rate of all the S15 mutants analysed, except F14S, was slower than that of the S15 control. Thus, saturation of this mRNA by the S15 protein mutants should occur.

This study provides a way of correlating results obtained with both the S15 RNA targets and allows the definition of the extent of mimicry between these two partners. It is thus possible to distinguish amino acids that are involved in both rRNA and mRNA binding from amino acids that specifically contact rRNA but not mRNA and, conversely, to identify amino acids that specifically recognize mRNA. A remarkable correlation is found between our results and those obtained with the mRNA substrate (Serganov *et al*., 2002) concerning the recognition of the G•U/G-C motif by amino acids His-41, Asp-48 and Ser-51. Taken together, our results indicate that the recognition of *rpsO* mRNA and 16S rRNA is similar but not identical. One of the most novel aspect of this study is the clear definition of a second subsite, which was suspected from footprinting experiments and mutagenesis data. Here, we show that Gly-22, Gln-27 and Thr-21, which are conserved in *Tt*-S15 and interact with two non-conserved basepairs (G750–C656 and C749–G657) in helix H22 of *Tt*-16S rRNA, are likely to be involved in the recognition of the distal part of stem S2 of the pseudoknot. *In vivo* (Bénard *et al*., 1994) and *in vitro* studies (Serganov *et al*., 2002) have shown that S15 binding to this subsite was sequence independent, suggesting that S15 mRNA recognition may rely more on a regular geometry of the helix backbone rather than on base sequence. This sequence flexibility was further demonstrated by the fact that the C(750)–G(656)/A(749)–U(657) basepairs of *Ec*-16S rRNA, and the G(750)–C(656)/C(749)–G(657) pairs of *Tt*-16S rRNA can all be recognized by Thr-21, Gly-22 and Gln-27 (Serganov *et al*., 2001). Thus, our results revealed an unsuspected potential mimicry that extends beyond the G•U/G-C recognition. Although not sequence specific, this type of mimicry takes advantage of a common topology: a regular helical portion located at a correct distance from the sequence-specific G•U/G-C motif.

The other new result is the evidence for specific contacts between S15 and its mRNA. Indeed, Arg-57, which does not participate in 16S rRNA recognition, plays a crucial role in autoregulation. This amino acid very likely interacts with A(−46), which occupies a unique

position in the pseudoknot. Specific recognition of mRNA relies on the recognition of this unique nucleotide crossing the deep major groove of the pseudoknot. Faced with the scarcity of determinants in the shallow groove of an RNA helix, this unusual position allows S15 to discriminate easily the specific shape of the pseudoknot required for autocontrol. As for Leu-38, another residue not involved in rRNA interaction, its proximity to nucleotide U(−49) in the pseudoknot raised the possibility of a specific contact at this position. Although the L38N (or the adjacent Q39L) mutation has a strong effect on autocontrol, the L38A mutation causes much less derepression, and no definitive conclusion can be drawn about the presence of a specific contact at this position.

Interestingly, the M58K mutation strongly increased the affinity of S15 for the pseudoknot *in vitro*, without leading to an increase in repression efficiency *in vivo*. This is not really surprising as the mechanism of regulation is not based on competition between 30S and mRNA, but on trapping the 30S subunit in an unproductive initiation complex, a mechanism that does not require high affinity (Schlax *et al*., 2001; Serganov *et al*., 2003). Thus, a new contact could be created without any major effect on fusion expression. On the other hand, it should be remembered that a major feature of autocontrol is the presence of ribosomes, which are not present in the *in vitro* binding experiments. *In vivo*, 30S subunits bind to the pseudoknot operator very efficiently to form a preternary initiation complex (Philippe *et al*., 1994). Binding of S15 to this complex prevents the formation of a productive initiation complex. It has been shown that, in addition to the Shine–Dalgarno sequence, the mRNA sequence located just downstream of the pseudoknot enhances both translation and repression efficiencies and, thus, binding of 30S subunits as well as binding by S15 (Philippe *et al*., 1993; 1994). It is thus possible that S15 also interacts with the 30S subunit and that some of the mutations described affect this potential interaction, accounting for some of the effects not described by the model.

In conclusion, this study shows that it is possible to isolate S15 mutants that have lost their ability to recognize mRNA while retaining their capacity for 16S rRNA binding. Two sets of determinants used for 16S rRNA binding are also involved in mRNA binding, indicating that some mimicry exists between the subsites of both targets. Nevertheless, other interactions are specifically devoted to mRNA recognition, suggesting that the observed mimicry is limited. Thus, *Ec*-S15 binds to its two targets using a common pattern and a set of specific determinants for each of them. This recognition mechanism differs from those described for some other ribosomal proteins. In these cases, either separate (L4: Li *et al*., 1996) or identical (S7: Robert and Brakier-Gingras, 2001; S8 and L1: Springer *et al*., 1998) RNA binding sites have been described. As the formation of a protein–RNA complex requires recognition in three dimensions, only a few specific contacts are required, which can be located at different positions in mRNA, obscuring the presence of mimicry in some cases (Serganov *et al*., 2003). Recent studies on L4 cast some doubt on the existence of true separate RNA binding sites on the same molecule (Stelzl *et al*., 2003). This work suggests that close structural similarity might exist in three dimensions between the mRNA and rRNA binding sites of the L4 protein, although these RNAs exhibit different secondary structures. Thus, mimicry might be the rule and distinct RNA structures, the exception, in the different examples of translational control.

One possible explanation is that targets that are less constrained are permitted to evolve more rapidly. rRNA, which is subjected to numerous constraints (i.e. it carries multiple binding sites), has a quite limited potential for evolution because mutations may have direct and/or indirect effects on rRNA folding and ribosomal protein binding sites. This is also true for ribosomal proteins, which must retain their specific contacts with rRNA. In contrast, evolution can occur more freely in mRNA leaders because they are not subjected to high stringency. This evolution can lead to changes in translation efficiency by interfering with ribosome loading. Two different types of translational control have been described (Draper, 1988). In the displacement model, the ribosomal protein competes with ribosomes for the occupation of mutually exclusive sites. Therefore, the repressor must bind mRNA with a much higher affinity than that for the 30S subunit or be in large excess over the 30S subunit (Schlax *et al*., 2001). Recognition of the ribosome binding site by the ribosomal protein has not been selected by evolution, probably because this site would not allow the specific recognition of a given mRNA. Taking advantage of the high affinity of ribosomal proteins for their cognate rRNA binding sites, evolution has selected the same determinants in mRNA leaders as those present in rRNA, thus creating a strong mimicry between these two kinds of RNA binding sites, as observed for the expression of *Ec*-threonyl-tRNA synthetase (Torres-Larios *et al*., 2002) or of *Tt*-S15 (Serganov *et al*., 2003). This situation contrasts with the entrapment model. In this case, no competition occurs between ribosomes and the repressor because their binding sites do not overlap. As shown for S4 and S15 mRNAs, the initiation codon is embedded in a pseudoknot that is stabilized after binding of the ribosomal protein and prevents the ribosome from accessing the start codon to the loading ribosome. In this case, only recognition of the pseudoknot is essential for autocontrol, and it must be selected by evolution while keeping the same affinity of the ribosomal protein for rRNA binding. This hypothesis accounts for the limited mimicry between mRNA and rRNA binding sites described in this paper. Although the affinity for the mRNA is quite low, it is, however, strong enough to recruit S15 and to stop translation. Thus, it appears that the mechanism selected to stop translation initiation determines the level of affinity required for the repressor to bind mRNA and then fixes the level of mimicry with the primary RNA binding site. Of course, the choice of mechanism should depend on the original RNA sequence and its structural potential.

Experimental procedures

Strains and cultures

The cells were grown in Luria–Broth (LB) medium as described by Miller (1972). IPTG was from Q-BIOgene (BIO101 Systems), ampicillin and chloramphenicol from Sigma and rifampicin from Ciba-Geigy. Strain AB5322 was derived from IBPC5321 (Robert-Le Meur and Portier, 1992) by double lysogenization with λ^+ and λ*rpsO–lacZ1* (Philippe *et al*., 1994).

Construction of a strain deleted for *rpsO*

Plasmid pBP111-4.2, a derivative of pBP111 (Portier *et al*., 1981; Portier, 1982) lacking *rpsO*, was kindly provided by Dr L. Bénard (unpublished data). In this plasmid, the *Sac*II–*Eco*O109I fragment overlapping *rpsO* was exchanged with a fragment carrying a

chloramphenicol-resistant cassette (Cm^R), thus creating a deletion of the entire *rpsO* gene and of a fragment encoding 81 amino acids of the upstream gene, *truB* (Nurse *et al*., 1995). The plasmid was linearized by *Hin*-dIII and used to transform strain CP7624, a lysogenic derivative of JC7623 (Jasin and Schimmel, 1984) carrying the *rpsO* gene in the λGF1 phage (Robert-Le Meur and Portier, 1992). The resulting transformant, JC7625, was grown at 30°C in LB and tested for its resistance to chloramphenicol (30 μg ml^{-1}) and sensitivity to ampicillin (100 μg ml^{-1}). The double cross-over event was confirmed by analysis of the polymerase chain reaction (PCR) products obtained from the chromosomal region carrying the deletion. A P1 lysate, obtained from this strain, was then used to transduce the lysogenic strain GF5321 (Robert-Le Meur and Portier, 1992), selecting for chloramphenicol resistance. Curing of the λ phage resulted in strain CPΔS15, which was unable to grow at 30°C, as expected for a strain lacking S15 (Yano and Yura, 1989). *recA56*, [*srl-300*::Tn*10*] was introduced into strain CPΔS15 by P1 transduction, and the resulting strain was then doubly lysogenized by λ^+ and λ*rpsO–lacZ1*. The final lysogen, CPFΔS15, which did not grow at 30°C, carried a translational fusion *rpsO–lacZ1* (Portier *et al*., 1990; Philippe *et al*., 1994) in which the reading frame of *rpsO* was restricted to the four first codons.

Construction of a plasmid expressing S15 under the control of an inducible promoter

Two restriction sites, *Nco*I and *Sal*I, were introduced at each end of the *rpsO* coding sequence, and this DNA fragment was cloned into the corresponding sites of plasmid pTrc99A (Amersham, GenBank accession number U13872), under the control of the inducible promoter p*Trc*. This promoter was repressed by the $lacI^q$ allele in the absence of IPTG (Fig. 1). In the resulting plasmid, designated pRPSO, transcription terminated at two strong terminators, T_1 and T_2, originating from the *rrnB* operon and located downstream of *rpsO*. In fact, insertion of the *rpsO* structural gene into the *Nco*I–*Sal*I sites of plasmid pTrc99A leads to expression of an S15 protein containing an alanine instead of a serine at the N-terminus and the addition of 21 amino acids at the C-terminus. To validate the results obtained with pRPSO, another plasmid, pRPSOWT, was constructed, which produced S15 with only a single additional arginine at its C-terminus (Fig. 3). In the presence of either pRPSO or pRPSOWT plasmid, the growth rates and the expression levels remained strictly identical, at 30°C and 42°C (data not shown), regardless of the presence of mutations. It can be concluded that, in the conditions used here, S15 can accommodate a long amino acid chain at its C-terminus without any effect on its interaction with its RNA targets. The two kinds of plasmids were thus used indiscriminately.

Mutagenesis

Site-directed mutagenesis was carried out according to the method of Kunkel (1985) on M13GF18, a M13mp18 derivative carrying the entire *rpsO* gene (Robert-Le Meur and Portier, 1992). After sequencing, a restriction fragment carrying the mutation was exchanged with the corresponding fragment of the wild-type *rpsO* gene carried by plasmid pRPSO or pRPSOWT.

Random mutagenesis was performed by PCR on 2 μg of pRPSO plasmid dissolved in 50 μl of *Taq* polymerase buffer (Appligene) containing 0.3 mM $MnCl_2$, 0.2 mM dNTP, 25 pmol of each oligonucleotide and 2 units of *Taq* polymerase. After 20 cycles (30 s at 93°C, 60 s at

55°C and 90 s at 72°C), the PCR fragments were digested by *Nco*I and *Sal*I restriction enzymes and ligated into the pRPSO or pRPSOWT plasmid, previously cut with the same enzymes. The resulting plasmids were used to transform strain CPFΔS15. Blue colonies growing at 30°C on Xgal plates containing 100 μg ml^{-1} ampicillin and 10^{-4} M IPTG were selected. Plasmid DNAs were purified from these clones, and the *rpsO* gene was sequenced to identify the mutations.

Protein-binding assays

The S15 mutants were expressed in *E. coli* BL21(DE3)Gold strain, using the pET29b vector (Novagene) according to the manufacturer's instructions (Stratagene). The overproduced S15 proteins represented the major protein fraction and were purified in two steps using ion-exchange chromatography on CM-Sepharose and gel filtration on Superdex 75. Ribosomes were removed before chromatography to reduce wild-type S15 content. Filter-binding assays were carried out as described previously (Serganov *et al*., 2002) with 1 h incubation on ice. No degradation of labelled RNA was detected during this incubation time. Binding of S15 to three *in vitro* transcribed RNAs was tested: a 304 nucleotide (nt) fragment from tmRNA, a 196 nt fragment from *Ec*-16S rRNA (Serganov *et al*., 1997) and a 47 nt fragment, corresponding to the minimum *Ec*-S15 mRNA pseudoknot (mRNA45) (Serganov *et al*., 2002) with two additional U and C nucleotides at the 3′ end. This RNA, designated mRNA47R53, was obtained after self-cleavage of the flanking hammerhead ribozymes and contained a 3′-cyclophosphate and no 5′-triphosphate. This RNA was shown to exhibit a higher affinity for *Ec*-S15 (K_d of 42 nM) than the larger mRNA fragment (K_d of 230 nM).

β-Galactosidase activity

Dosage of β-galactosidase level was measured according to the method of Miller (1972) in cells grown in LB medium in the presence 10^{-4} M IPTG, at either 30°C or 42°C.

S15 degradation assay

Cultures were grown to mid-logarithmic phase in LB medium either in the absence (42°C) or in the presence (30°C) of 10^{-4} M IPTG. S15 synthesis was induced with 2×10^{-3} M IPTG for 30 min. Then, chloramphenicol (100 μg ml^{-1}) and rifampicin (300 μg ml^{-1}) were added, and 2 ml aliquots of the cultures were taken at the times indicated. The cells were precipitated with cold 10% trichloracetic acid, washed with acetone, dried, resuspended in SDS sample buffer (30 mM Tris-HCl, pH 6.8, 1% SDS, 0.14 β-mercaptoethanol, 20% glycerol and bromophenol blue) and heated at 95°C for 2 min. The samples were run on 15% SDS-polyacrylamide gels, transferred onto a nitrocellulose membrane (Hybond-C® Extra; Amersham) in 25 mM AMPSO, pH 9.5, containing 20% methanol overnight at 150 mA in a FEB20 electroblotting unit (Fisherbrand). The protein was visualized with an anti-S15 antibody (Agro-Bio) and [^{125}I]-protein A (37 kBq at 1.11 GBq mg^{-1}; Amersham). Quantification of the S15 band intensity was performed with a PhosphorImager.

Computer modelling

The *Ec*-mRNA–S15 complex was derived from the previously built model (Serganov *et al*., 2002) using program O (Jones *et al*., 1991). Figures were drawn with VIEWEELITE (Accelerys).

Acknowledgements

We thank L. Bénard for the gift of plasmid pBP111-4.2. E. Ennifar and P. Dumas are thanked for helpful discussions and suggestions, and we are indebted to P. Dumas for improvement of the computer model. We acknowledge C. Condon for careful reading and suggestions for improvement of the manuscript. This research was supported by the CNRS (UPR9073, UPR9002) and by NIH grant CA46778 to D.P.

References

1. Agalarov SC, Sridhar Prasad G, Funke PM, Stout CD, Williamson JR. Structure of the S15,S6,S18-rRNA complex: assembly of the 30S ribosome central domain. Science. 2000; 288:107–113. [PubMed: 10753109]
2. Batey RT, Williamson JR. Interaction of the *Bacillus stearothermophilus* ribosomal protein S15 with 16 S rRNA. I. Defining the minimal RNA site. J Mol Biol. 1996a; 261:536–549. [PubMed: 8794875]
3. Batey RT, Williamson JR. Interaction of the *Bacillus stearothermophilus* ribosomal protein S15 with 16 S rRNA. II. Specificity determinants of RNA-protein recognition. J Mol Biol. 1996b; 261:550–567. [PubMed: 8794876]
4. Bénard L, Philippe C, Dondon L, Grunberg-Manago M, Ehresmann B, Ehresmann C, Portier C. Mutational analysis of the pseudoknot structure of the S15 translational operator from *Escherichia coli*. Mol Microbiol. 1994; 14:31–40. [PubMed: 7830558]
5. Bénard L, Mathy N, Grunberg-Manago M, Ehresmann B, Ehresmann C, Portier C. Identification in a pseudoknot of a UG motif essential for the regulation of the expression of ribosomal protein S15. Proc Natl Acad Sci USA. 1998; 95:2564–2567. [PubMed: 9482926]
6. Dabbs ER. Mutants lacking individual ribosomal proteins as a tool to investigate ribosomal properties. Biochimie. 1991; 73:639–645. [PubMed: 1837238]
7. Draper, DE. Translational regulation of ribosomal proteins in *Escherichia coli*. In: Ilan, J., editor. Translational Control of Gene Expression. New York: Plenum Press; 1988. p. 1-26.
8. Ferro-Novick S, Honma M, Beckwith J. The product of gene *secC* is involved in the synthesis of exported proteins in *E. coli*. Cell. 1984; 38:211–217. [PubMed: 6088066]
9. Jasin M, Schimmel P. Deletion of an essential gene in *Escherichia coli* by site-specific recombination with linear DNA fragments. J Bacteriol. 1984; 159:783–786. [PubMed: 6086588]
10. Jones TA, Zou JY, Cowan SW, Kjeldgaard M. Improved methods for building protein models in electron density maps and the location of errors in these models. Acta Crystallogr A. 1991; 47:110–119. [PubMed: 2025413]
11. Kunkel TA. Rapid and efficient site-specific mutagenesis without phenotypic selection. Proc Natl Acad Sci USA. 1985; 82:488–492. [PubMed: 3881765]
12. Li X, Lindahl L, Zengel JM. Ribosomal protein L4 from *Escherichia coli* utilizes nonidentical determinants for its structural and regulatory functions. RNA. 1996; 2:24–37. [PubMed: 8846294]
13. Miller, JH. Experiments in Molecular Genetics. Cold Spring Harbor, NY: Cold Spring Harbor Laboratory Press; 1972.
14. Nikulin A, Serganov A, Ennifar E, Tishchenko S, Nevskaya N, Shepard W, et al. Crystal structure of the S15–rRNA complex. Nature Struct Biol. 2000; 7:273–277. [PubMed: 10742169]
15. Nishi K, Schnier J. The phenotypic suppression of a mutation in the gene *rplX* for ribosomal protein L24 by mutations affecting the *lon* gene product for protease LA in *Escherichia coli* K12. Mol Gen Genet. 1988; 212:177–181. [PubMed: 3287098]
16. Nurse K, Wrzesinski J, Bakin A, Lane BG, Ofengand J. Purification, cloning, and properties of the tRNA psi 55 synthase from *Escherichia coli*. RNA. 1995; 1:102–112. [PubMed: 7489483]

17. Olsson MO, Isaksson LA. Analysis of *rpsD* mutations in *Escherichia coli*. III. Effects of *rpsD* mutations on expression of some ribosomal protein genes. Mol Gen Genet. 1979; 169:271–278. [PubMed: 372749]
18. Petersen C. *Escherichia coli* ribosomal protein L10 is rapidly degraded when synthesized in excess of ribosomal protein L7/L12. J Bacteriol. 1990; 172:431–436. [PubMed: 2403546]
19. Philippe C, Portier C, Mougel M, Grunberg-Manago M, Ebel J-P, Ehresmann B, Ehresmann C. Target site of *Escherichia coli* ribosomal protein S15 on its messenger RNA. Conformation and interaction with the protein. J Mol Biol. 1990; 211:415–426. [PubMed: 2407855]
20. Philippe C, Eyermann F, Bénard L, Portier C, Ehresmann B, Ehresmann C. Ribosomal protein S15 from *Escherichia coli* modulates its own translation by trapping the ribosome on the mRNA initiation loading site. Proc Natl Acad Sci USA. 1993; 90:4394–4398. [PubMed: 7685101]
21. Philippe C, Bénard L, Eyermann F, Cachia C, Kirillov SV, Portier C, et al. Structural elements of *rps0* mRNA involved in the modulation of translational initiation and regulation of *E. coli* ribosomal protein S15. Nucleic Acids Res. 1994; 22:2538–2546. [PubMed: 8041615]
22. Philippe C, Bénard L, Portier C, Westhof E, Ehresmann B, Ehresmann C. Molecular dissection of the pseudoknot governing the translational regulation of *Escherichia coli* ribosomal protein S15. Nucleic Acids Res. 1995; 23:18–28. [PubMed: 7532857]
23. Portier C. Physical localisation and direction of transcription of the structural gene for *Escherichia coli* ribosomal protein S15. Gene. 1982; 18:261–266. [PubMed: 6290330]
24. Portier C, Migot C, Grunberg-Manago M. Cloning of *E. coli pnp* gene from an episome. Mol Gen Genet. 1981; 183:298–305. [PubMed: 6276682]
25. Portier C, Dondon L, Grunberg-Manago M. Translational autocontrol of the *Escherichia coli* ribosomal protein S15. J Mol Biol. 1990; 211:407–414. [PubMed: 2407854]
26. Robert F, Brakier-Gingras L. Ribosomal protein S7 from *Escherichia coli* uses the same determinants to bind 16S ribosomal RNA and its messenger RNA. Nucleic Acids Res. 2001; 29:677–682. [PubMed: 11160889]
27. Robert-Le Meur M, Portier C. *E. coli* polynucleotide phosphorylase expression is autoregulated through an RNase III-dependent mechanism. EMBO J. 1992; 11:2633–2641. [PubMed: 1628624]
28. Romby P, Springer M. Bacterial translational control at atomic resolution. Trends Genet. 2003; 19:155–161. [PubMed: 12615010]
29. Schlax PJ, Xavier KA, Gluick TC, Draper DE. Translational repression of the *Escherichia coli* alpha operon mRNA: importance of an mRNA conformational switch and a ternary entrapment complex. J Biol Chem. 2001; 276:38494–38501. [PubMed: 11504736]
30. Scott LG, Williamson JR. Interaction of the *Bacillus stearothermophilus* ribosomal protein S15 with its 5′-translational operator mRNA. J Mol Biol. 2001; 314:413–422. [PubMed: 11846555]
31. Serganov AA, Masquida B, Westhof E, Cachia C, Portier C, Garber M, et al. The 16S rRNA binding site of *Thermus thermophilus* ribosomal protein S15: comparison with *Escherichia coli* S15, minimum site and structure. RNA. 1996; 2:1124–1138. [PubMed: 8903343]
32. Serganov A, Rak A, Garber M, Reinbolt J, Ehresmann B, Ehresmann C, et al. Ribosomal protein S15 from *Thermus thermophilus*: cloning, sequencing, overexpression of the gene and RNA-binding properties of the protein. Eur J Biochem. 1997; 246:291–300. [PubMed: 9208917]
33. Serganov A, Bénard L, Portier C, Ennifar E, Garber M, Ehresmann B, Ehresmann C. Role of conserved nucleotides in building the 16S rRNA binding site for ribosomal protein S15. J Mol Biol. 2001; 305:785–803. [PubMed: 11162092]
34. Serganov A, Ennifar E, Portier C, Ehresmann B, Ehresmann C. Do mRNA and rRNA binding sites of *E. coli* ribosomal protein S15 share common structural determinants? J Mol Biol. 2002; 320:963–978. [PubMed: 12126618]
35. Serganov A, Polonskaia A, Ehresmann B, Ehresmann C, Patel DJ. Ribosomal protein S15 represses its own translation *via* adaptation of rRNA-like fold within its mRNA. EMBO J. 2003; 22:1–11. [PubMed: 12505979]
36. Springer M, Plumbridge JA, Butler JS, Graffe M, Dondon J, Mayaux JF, et al. Autogenous control of *Escherichia coli* threonyl-tRNA synthetase expression *in vivo*. J Mol Biol. 1985; 185:93–104. [PubMed: 3930755]

37. Springer, M.; Portier, C.; Grunberg-Manago, M. RNA mimicry in the translational apparatus. In: Simons, RW.; Grunberg-Manago, M., editors. RNA Structure and Function. New York: Cold Spring Laboratory Press; 1998. p. 377-413.

38. Stelzl U, Zengel JM, Tovbina M, Walker M, Nierhaus KH, Lindahl L, Patel DJ. RNA-structural mimicry in *Escherichia coli* ribosomal protein L4-dependent regulation of the *S10* operon. J Biol Chem. 2003; 278:28237–22845. [PubMed: 12738792]

39. Torres-Larios A, Dock-Bregeon AC, Romby P, Rees B, Sankaranarayanan R, Caillet J, et al. Structural basis of translational control by *Escherichia coli* threonyl tRNA synthetase. Nature Struct Biol. 2002; 9:343– 347. [PubMed: 11953757]

40. Vanzo NF, Li YS, Py B, Blum E, Higgins CF, Raynal LC, et al. Ribonuclease E organizes the protein interactions in the *Escherichia coli* RNA degradosome. Genes Dev. 1998; 12:2770–2781. [PubMed: 9732274]

41. Yano R, Yura T. Suppression of the *Escherichia coli rpoH* opal mutation by ribosomes lacking S15 protein. J Bacteriol. 1989; 171:1712–1717. [PubMed: 2646293]

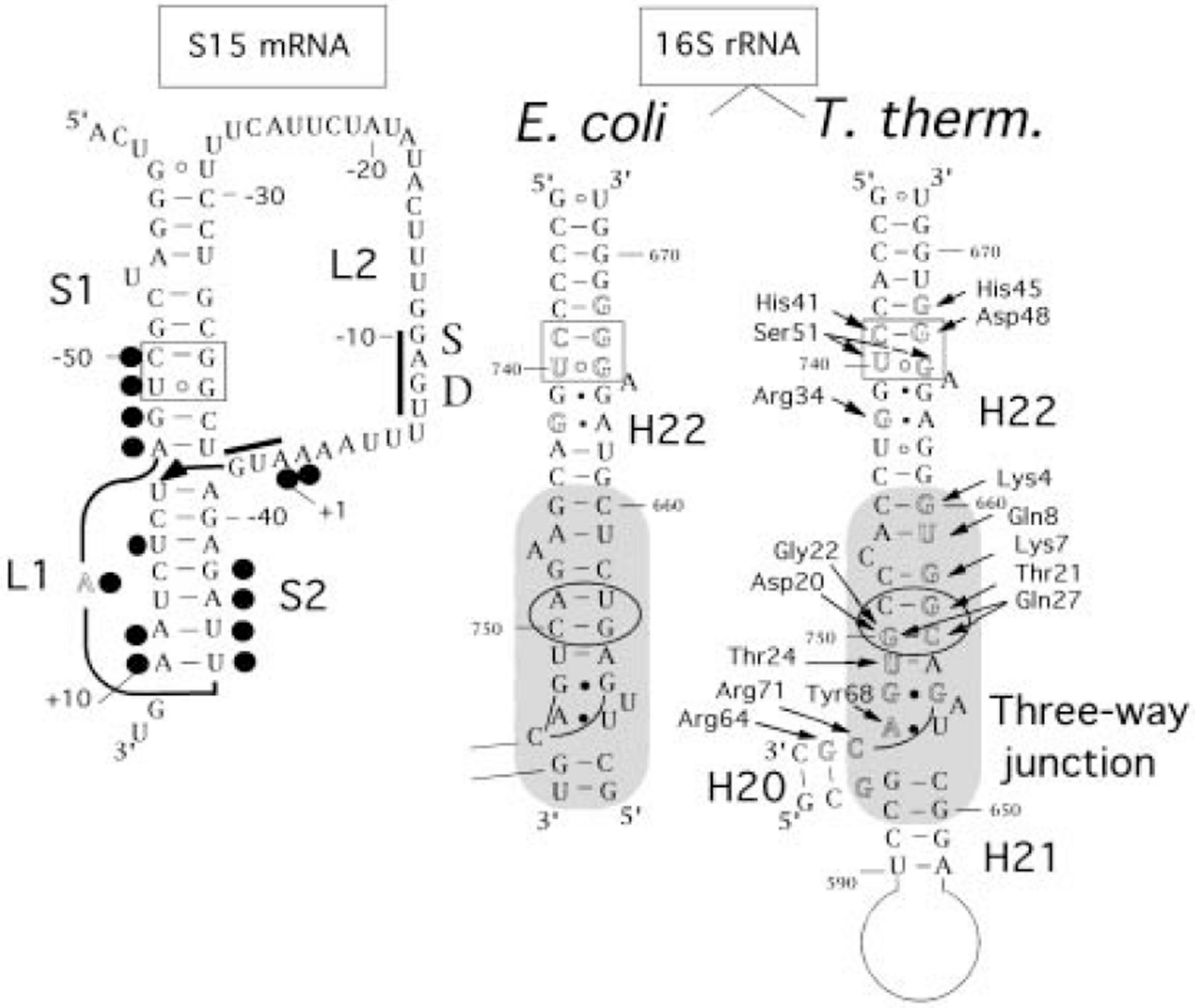

Fig. 1.

Secondary structure of the S15 targets. The U•G/C-G motif common to both targets is framed, and the putative second binding subsite is circled.

S15 mRNA: the initiation codon and the Shine–Dalgarno sequence are underlined. Black dots show the nucleotides protected by S15 from hydroxyl radical cleavage (Philippe *et al*., 1995).

16S rRNA: nucleotides interacting with amino acids of S15 in the three-dimensional structure of the *Tt*-16S rRNA–S15 complex (Nikulin *et al*., 2000) are shown in outlined characters. Most of the amino acids of *Tt*-S15 found to contact rRNA in the complex are indicated. The major S15 binding site of *Tt*-rRNA and the corresponding region of *Ec*-rRNA are shaded.

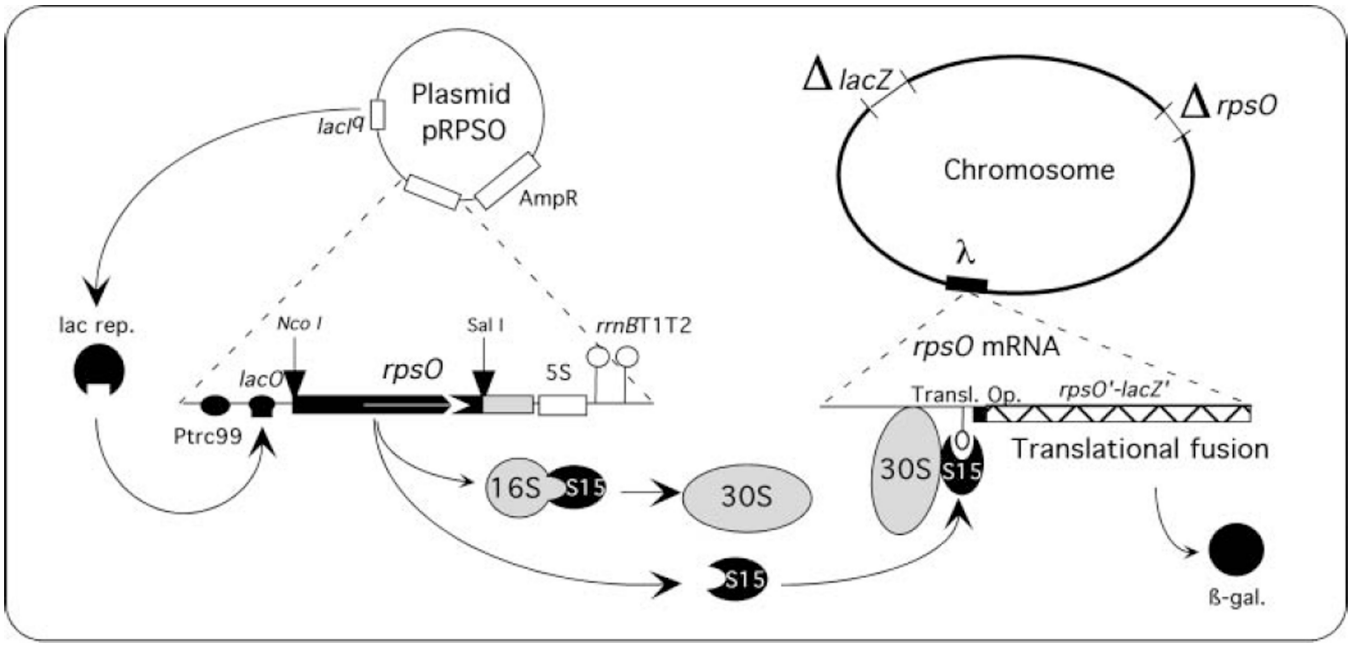

Fig. 2.

Strategy to investigate the effects of S15 mutations on autorepression. The *rpsO* gene, encompassed by the *Nco*I and *Sal*I restriction sites of the pRPSO plasmid, is expressed in the presence of IPTG. Overproduced S15 first binds 16S rRNA and then the translational operator (Transl. Op.), located upstream of a *rpsO–lacZ* translational fusion that is inserted into the chromosome of strain CPFΔS15. Interaction of S15 with mRNA prevents translation initiation, resulting in poor translation of the fusion detected by β-galactosidase assay. The plasmid carries the ampicillin resistance gene (Amp^R) and the $lacI^q$ gene, encoding the *lac* repressor (lac rep.). The *rpsO* gene is enlarged. Ptrc99, promoter of *rpsO*; $lacI^q$, gene of *lac* repressor (lac rep.); *lacO*, *lac* repressor; 5S, 5S rRNA; rrn*B*T1T2, transcriptional terminators of the rRNA gene. The *lacZ* and *rpsO* deletions in the chromosome are shown by thin lines. The λ phage carrying the translational fusion is indicated by a black bar, and the corresponding chimeric messenger RNA transcribed from the *rpsO* promoter is shown enlarged. The black square corresponds to the first four codons of the *rpsO* gene fused to *lacZ* (crossed bar).

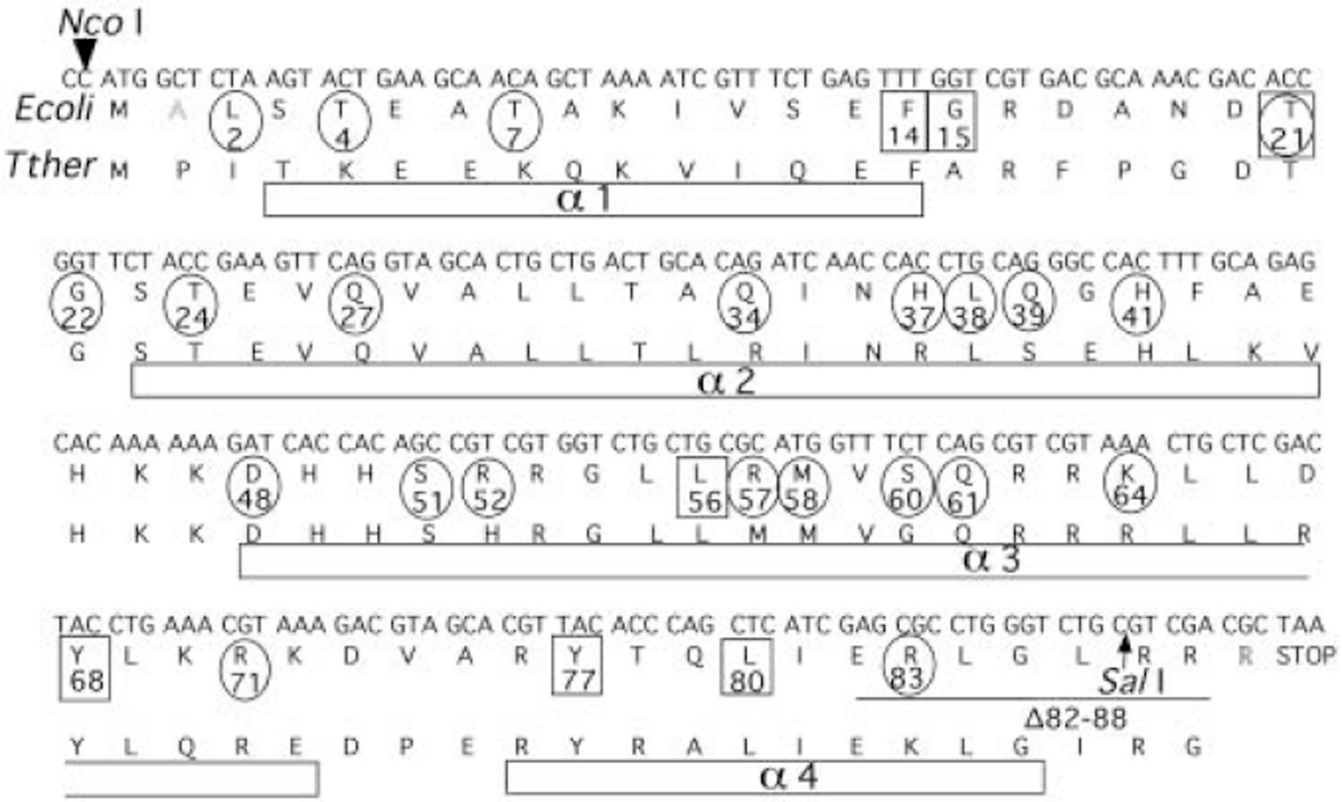

Fig. 3.

Location of the mutations studied. Sequences of the *rpsO* gene in *E. coli* and *T. thermophilus* are given for comparison. The insertion points of the *Nco*I–*Sal*I fragment carrying the *rpsO* gene in the pTrc99A plasmid are indicated. Directed (circles) and selected (rectangles) mutations are numbered as in Table 1. Bars correspond to α-helices.

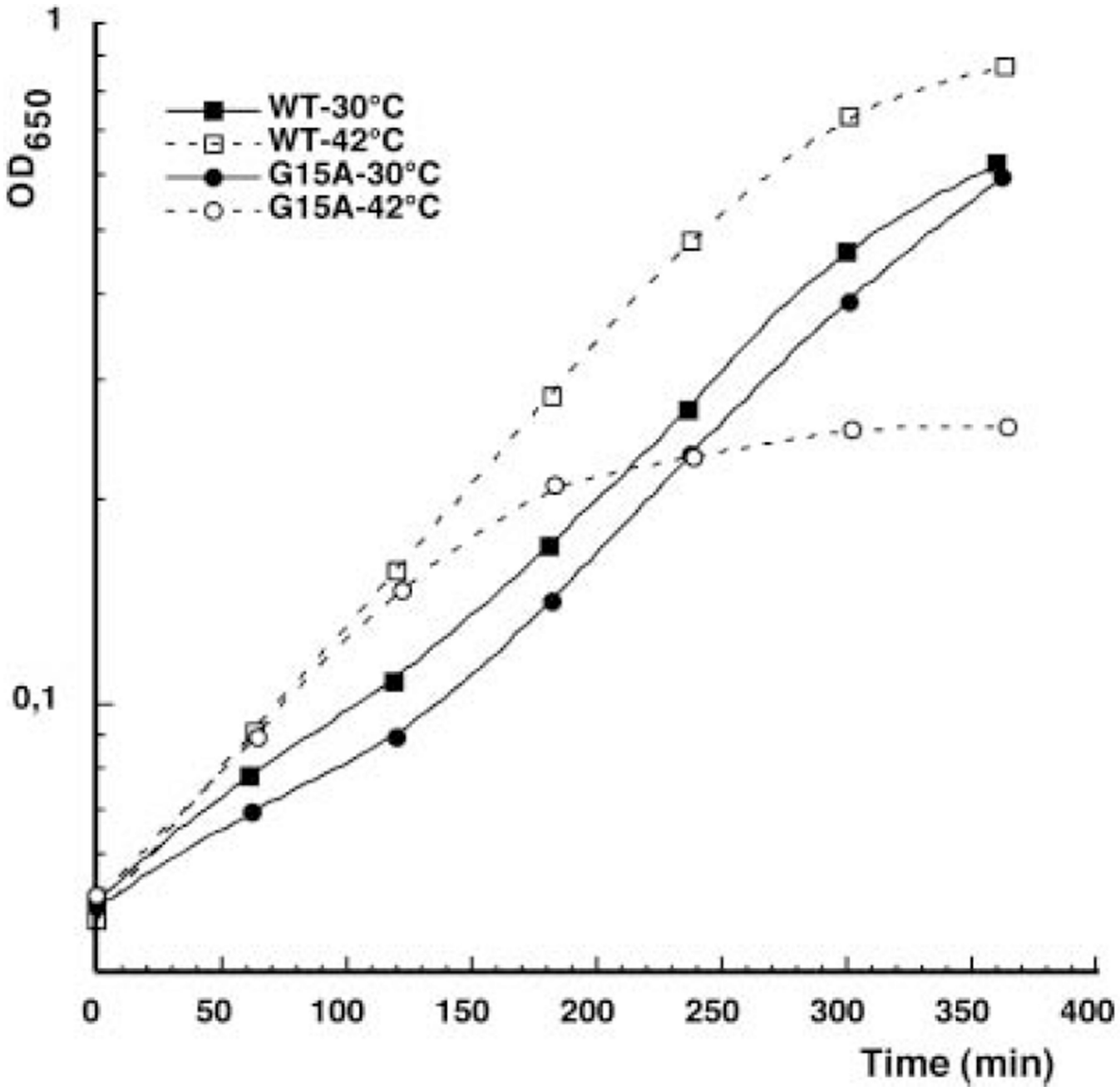

Fig. 4.

Effect of temperature on the growth rate of strain CPFΔS15 carrying the G15A mutation. Cells were grown in Luria broth medium at 30°C and 42°C. At the time indicated, aliquots were taken to measure the optical density (OD_{650}) of the culture. Black symbols correspond to culture at 30°C, and void symbols to culture at 42°C. Squares, wild-type S15 (WT); circles, S15 mutant (G15A).

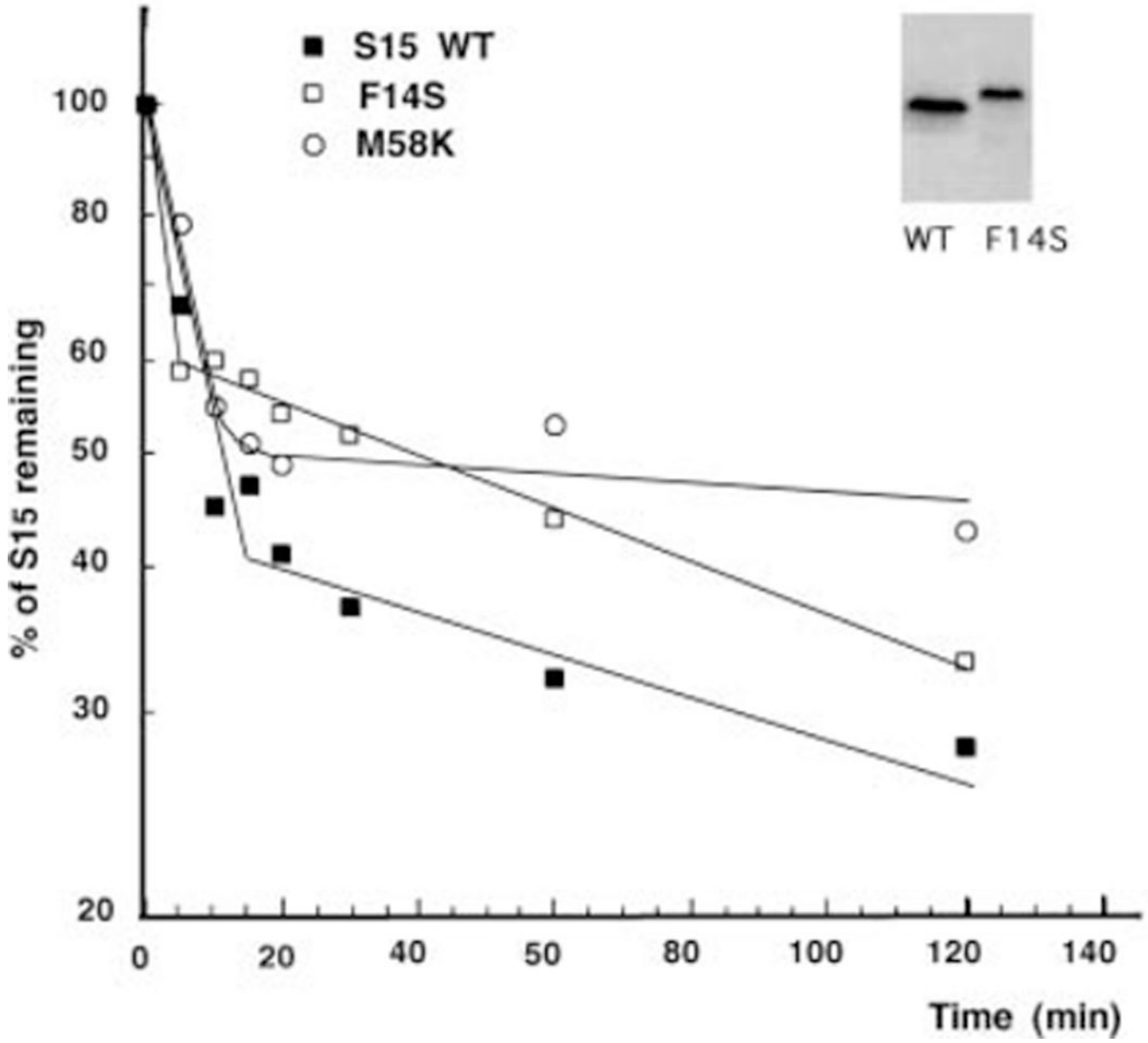

Fig. 5.

Decay rate of the S15 mutants. Aliquots of bacterial cultures expressing S15 were taken at different times after the addition of rifampicin and chloramphenicol. The proteins were separated on an SDS-polyacrylamide gel, immunoblotted with anti-S15 antibodies and treated with radioactively labelled protein A. The amount of S15 was quantified by PhosphorImager and plotted versus time. Inset: migration rate of the F14S mutant. WT, wild-type S15.

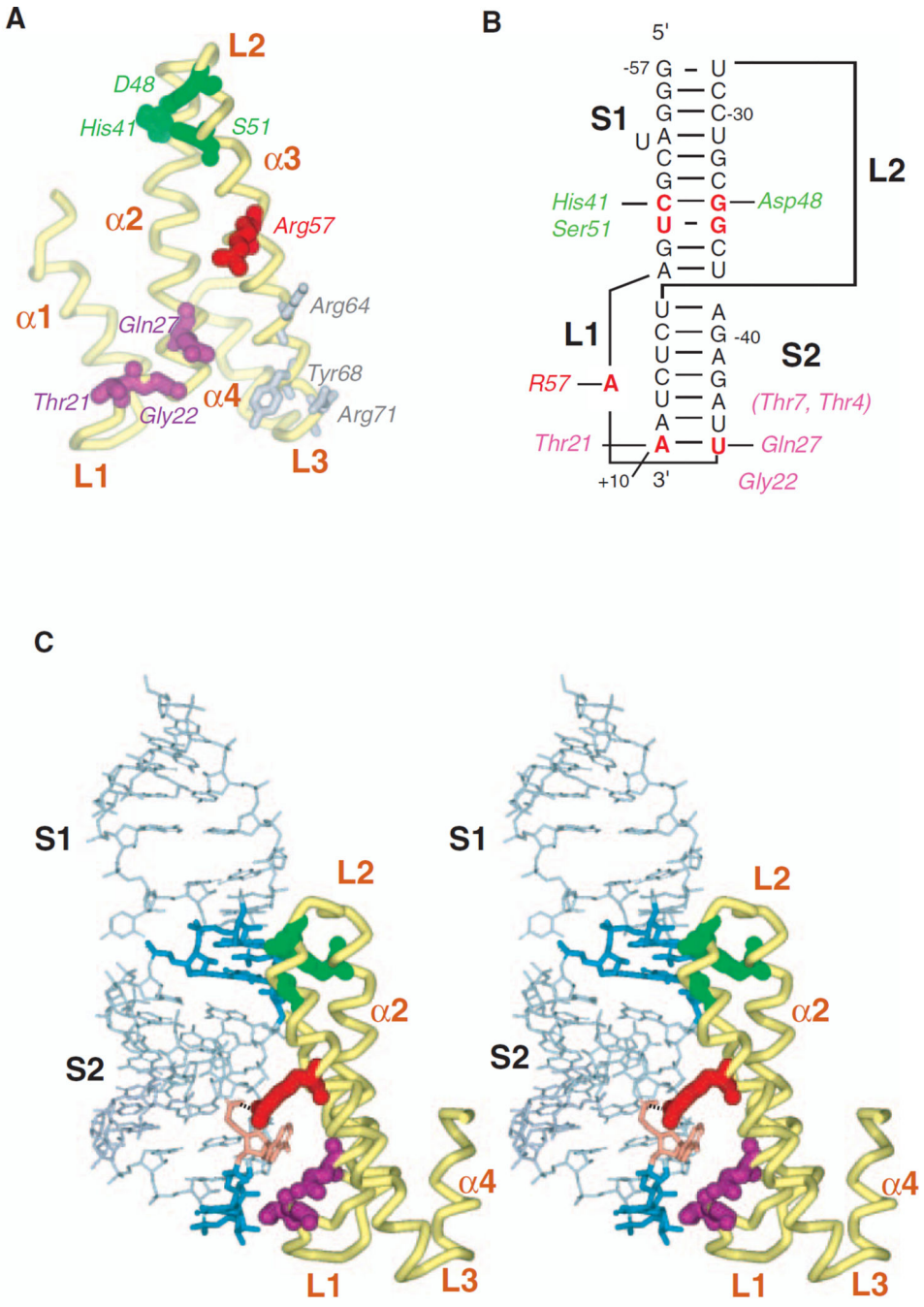

Fig. 6.

Interactions between *E*c-S15 and its target mRNA.

A. S15 protein. Protein backbone is shown by a tube. The lateral chains of amino acids essential for autocontrol are shown in colour: green for conserved amino acids that recognize the G•U/G-C motif in both *Tt*-16S rRNA and mRNA; violet for conserved amino acids that interact with stem S2 of the pseudoknot and helix H22 of *Tt*-16S rRNA; and red for Arg-57 that interacts specifically with mRNA and not 16S rRNA. Those amino acids that interact with the 16S rRNA three-way junction but not with mRNA are shown in grey.

B. Pseudoknot. The nucleotides interacting with S15 are shown in red. Loop L2 carrying the initiation codon and the Shine–Dalgarno sequence is schematized by a line. Loop L1 is represented by a unique nucleotide A(−46) crossing the deep narrow groove and bulging out. Amino acids interacting with mRNA are indicated, with the same colour code as in (A). C. Three-dimensional model of the S15–mRNA complex. In this stereoimage, RNA is shown in grey, with stems S1 and S2 co-axially stacked (loop L2 being omitted). The nucleotides interacting with S15 through amino acids also recognized by 16S rRNA are highlighted in blue. The bulged A(−46), specifically recognized by *Ec*-S15, is shown in light red. The stacking of Arg-57 on the adenine base ring is visible, and the possible contact with the phosphate group is indicated by a dashed line. The protein is represented as in (A) with the same colour code used for amino acids.

Table 1

Repression of the *rpsO–lacZ* fusion by different S15 mutants.

***Tt*-aa**	***Tt-r*RNA contacts**	***Ec*-aa mut.**	**Units (30°C)**	**R**	**Units (42°C)**	**R**	**Possible contact with mRNA**
		CPFΔS15			9 092 ± 235		
		+pTrc99A			9 863 ± 565		
		+pRPSO	26 ± 5	379	46 ± 7	214	
F14		**F14S**	8 378 ± 700	1	14 775 ± 1457	1	
T21	G657(N2,O2′)	**T21A**	4 057 ± 271	2	8 270 ± 1079	1	A(−43)(N3)
G22	G750(N2,O2′)	G22A	11 118 ± 492	1	10 044 ± 112	1	Contact with S2 (?)
L38		L38N	5 490 ± 631	2	11 957 ± 377	1	Possible
		L38A	2 589 ± 861	4	1 707 ± 747	6	specific contact
S39		**Q39L**	4 160 ± 1610	2	14 124 ± 1021	1	Leu → altered
		Q39A	73 ± 1	135	121 ± 42	82	conformation
H41	C739(O2,O2′)	H41A	12 487 ± 657	1	10 500 ± 377	1	C(−50) (O2,O2′)
D48	G667(N2,N3)	D48G	13 923 ± 556	1	17 119 ± 244	1	G(−35)(N2,N3)
	U740(O2′)						
S51	w-G666(N2)	S51L	10 720 ± 220	1	11 720 ± 2542	1	Leu → steric clash
	U740(O2)	S51A	62 ± 7	159	46 ± 6	214	
L56		**L56P**	7 683 ± 252	1	9 200 ± 135	1	Pro → altered
		L56A	101 ± 10	98	100 ± 25	99	conformation
		R57A	4 633 ± 247	2	8 250 ± 752	1	
		R57Q	3 048 ± 252	3	7 753 ± 1028	1	Specific contact
M57		R57N	850 ± 58	12	2 643 ± 305	4	
		R57H	367 ± 17	27	1 811 ± 362	5	(5′PO4 A(−46) + stacking on base ring)
		R57K	215 ± 11	46	594 ± 61	17	
		R57A,M58K	214 ± 9	46	1 518 ± 136	7	
M58		M58K	51 ± 7	193	41 ± 7	241	
Q27	C656(O2′)	Q27R	889 ± 176	11	2 668 ± 84	3	U(−45)(O2′)
	G750(N2)	Q27A	1 497 ± 95	7	3 035 ± 298	3	
		Δ82–88	1 064 ± 33	9	3 493 ± 452	3	

Tt-aa	*Tt-r*RNA contacts	*Ec*-aa mut.	Units (30°C)	R	Units (42°C)	R	Possible contact with mRNA
K4	5′PO4-G660	T4A	510 ± 69	19	261 ± 47	38	Contacts with S2 (?)
K7	5′PO4-G658	T7A	634 ± 3	16	470 ± 45	21	Contacts with S2 (?)
A15		G15A	611 ± 8	16	No growth		
L80		**L80F**	515 ± 33	19	699 ± 63	14	No contact
I2		**L2P**	56 ± 3	176	123 ± 7	80	
T24	U751(O2′)	T24S	44 ± 7	224	126 ± 23	78	No contact
		T24A	54 ± 12	182	52 ± 11	190	
R34	5′PO4-G742	Q34A	68 ± 1	145	118 ± 21	84	No contact
N36		N36A	140 ± 11	70	114 ± 4	87	
R37		H37A	92 ± 6	107	254 ± 154	39	Conform./stability
H52		R52A	124 ± 2	80	135 ± 8	73	
G60		S60A	82 ± 11	120	68 ± 12	145	
Q61		Q61A	63 ± 1	156	137 ± 5	72	
R64	5′PO4-G755	K64A	116 ± 15	85	244 ± 48	40	No contact
Y68	5′PO4-A753	**Y68N**	137 ± 29	72	204 ± 72	48	
		Y68A	24 ± 2	411	104 ± 6	95	No contact
R71	5′PO4-G754	R71A	35 ± 4	282	104 ± 6	95	No contact
Y77		**Y77C**	26 ± 1	379	61 ± 13	162	
K83		R83A	32 ± 1	308	93 ± 12	106	

Wild-type S15 was produced from the pRPSO plasmid in the presence of 10^{-4} M IPTG in a strain lacking the chromosomal S15 gene (Δ*rpsO*), and expression of the fusion was measured at 30°C and 42°C. Control, no plasmid; pTrc99A, empty vector; pRPSO, pTrc99A derivative carrying *rpsO*. Random mutations are shown in bold characters. Identity of *Tt*-S15 amino acids (*Tt*-aa) corresponding to the same position as mutated *Ec*-S15 amino acids (*Ec*-aa mut) are indicated. Contacts between *Tt*-residues and 16S rRNA in the *Tt*-rRNA–S15 complex are also described. R, repression factor [corresponding to the ratio between β-galactosidase values in the absence (pTrc99A) and in the presence of S15]. Heavy horizontal bars define four classes of repression efficiency. From top to bottom: 4000–10000 units, null; 4000–1000, weak; 1000–250, strong; 250–0, complete. The potential contacts with mRNA are described, and possible effects on conformation are indicated.

Table 2

Apparent equilibrium dissociation constants for the S15 mutants binding to 16S rRNA and to S15 translational operator (pseudoknot).

	$K_d \times 10^{-9}$ M					
S15 mutations	**WT**	**F14L**	**R57A**	**R57K**	**R57A/R57K**	**M58K**
Control (tmRNA)	>10 000	>20 000	50 000	10 000	10 000	>40 000
16S rRNA	2.4 ± 0.3	7.2 ± 0.4	9.6 ± 0.2	2.6 ± 0.4	4.8 ± 0.7	0.96 ± 0.7
S15 mRNA	42 ± 22	572 ± 115	1150 ± 350	1020 ± 300	1340 ± 230	5.9 ± 1.4